REPORT DOCUMENTATION PAGE

Form Approved OMB NO. 0704-0188

1. REPORT DATE (DD-MM-YYYY)	2. REPORT TYPE	3. DATES COVERED (From - To)
22-12-2015	Final Report	1-Jan-2015 - 30-Sep-2015

4. TITLE AND SUBTITLE

Final Report: STIR Proposal For Research Area 2.1.2 Surface Energy Balance: Transient Soil Density Impacts Land Surface Characteristics And Characterization

5a. CONTRACT NUMBER
W911NF-14-1-0655

5b. GRANT NUMBER

5c. PROGRAM ELEMENT NUMBER
611102

5d. PROJECT NUMBER

5e. TASK NUMBER

5f. WORK UNIT NUMBER

6. AUTHORS

Joshua L. Heitman

7. PERFORMING ORGANIZATION NAMES AND ADDRESSES

North Carolina State University
2701 Sullivan Drive
Admin Services III; Box 7514
Raleigh, NC 27695 -7514

8. PERFORMING ORGANIZATION REPORT NUMBER

9. SPONSORING/MONITORING AGENCY NAME(S) AND ADDRESS (ES)

U.S. Army Research Office
P.O. Box 12211
Research Triangle Park, NC 27709-2211

10. SPONSOR/MONITOR'S ACRONYM(S)
ARO

11. SPONSOR/MONITOR'S REPORT NUMBER(S)
66053-EV-II.2

12. DISTRIBUTION AVAILIBILITY STATEMENT

Approved for Public Release; Distribution Unlimited

13. SUPPLEMENTARY NOTES

The views, opinions and/or findings contained in this report are those of the author(s) and should not contrued as an official Department of the Army position, policy or decision, unless so designated by other documentation.

14. ABSTRACT

Soil density is commonly treated as static in studies on land surface property dynamics. Magnitudes of errors associated with this assumption are largely unknown. Objectives of this preliminary investigation were to: i) quantify effects of soil density variation on soil properties, and ii) evaluate impact of changing soil density on surface energy balance and heat and water transfer. Six soil properties were evaluated over a range of soil densities, using a combination of ten modeling approaches. Thermal conductivity, water characteristics, hydraulic

15. SUBJECT TERMS

Soil, hydrology, surface energy balance

16. SECURITY CLASSIFICATION OF:			17. LIMITATION OF ABSTRACT	15. NUMBER OF PAGES	19a. NAME OF RESPONSIBLE PERSON
a. REPORT	b. ABSTRACT	c. THIS PAGE			Joshua Heitman
UU	UU	UU	UU		19b. TELEPHONE NUMBER 919-513-1593

Standard Form 298 (Rev 8/98)
Prescribed by ANSI Std. Z39.18

Report Title

Final Report: STIR Proposal For Research Area 2.1.2 Surface Energy Balance: Transient Soil Density Impacts Land Surface Characteristics And Characterization

ABSTRACT

Soil density is commonly treated as static in studies on land surface property dynamics. Magnitudes of errors associated with this assumption are largely unknown. Objectives of this preliminary investigation were to: i) quantify effects of soil density variation on soil properties, and ii) evaluate impact of changing soil density on surface energy balance and heat and water transfer. Six soil properties were evaluated over a range of soil densities, using a combination of ten modeling approaches. Thermal conductivity, water characteristics, hydraulic conductivity, and vapor diffusivity were most sensitive; these properties changed by fractions greater than associated change in density (i.e., 10% change in density led to >10% change in property). Subsequently, three field seasons were simulated with a numerical model (HYDRUS-1D) for a range of bulk densities. Among the surface energy balance terms, ground heat flux and latent heat flux were most sensitive to bulk density. Surface soil temperature variation increased in with low bulk densities but subsurface temperature variation decreased. Surface water content varied with bulk density but effects mostly disappeared in the subsurface. Results demonstrate significance of transient density on surface conditions and point to need for continued evaluation of impacts with improved measurements and modeling.

Enter List of papers submitted or published that acknowledge ARO support from the start of the project to the date of this printing. List the papers, including journal references, in the following categories:

(a) Papers published in peer-reviewed journals (N/A for none)

Received Paper

TOTAL:

Number of Papers published in peer-reviewed journals:

(b) Papers published in non-peer-reviewed journals (N/A for none)

Received Paper

TOTAL:

Number of Papers published in non peer-reviewed journals:

(c) Presentations

Kojima, Y., J.L. Heitman, and R. Horton. 2015. Numerical Evaluation of Transient Density Impact on Surface Energy Balance and Coupled Heat and Water Transfer in Soils. Grand Challenges in Modeling Soil Processes. Soil Science Society of America International Meeting, Minneapolis, MN. November 16, 1015.

Number of Presentations: 1.00

Non Peer-Reviewed Conference Proceeding publications (other than abstracts):

Received Paper

TOTAL:

Number of Non Peer-Reviewed Conference Proceeding publications (other than abstracts):

Peer-Reviewed Conference Proceeding publications (other than abstracts):

Received Paper

TOTAL:

Number of Peer-Reviewed Conference Proceeding publications (other than abstracts):

(d) Manuscripts

Received		Paper
12/22/2015	1.00	Lalit Arya, Joshua Heitman. A Non-Empirical Method for Computing Pore Radii and Soil Water Characteristics from Particle-Size Distribution, Soil Science Society of America Journal (04 2015)

TOTAL: **1**

Number of Manuscripts:

Books

Received	Book

TOTAL:

Received	Book Chapter

TOTAL:

Patents Submitted

Patents Awarded

Awards

Graduate Students

NAME	PERCENT_SUPPORTED
FTE Equivalent:	
Total Number:	

Names of Post Doctorates

NAME	PERCENT_SUPPORTED
Xinhua Xiao	0.75
Yuki Kojima	0.00
FTE Equivalent:	**0.75**
Total Number:	**2**

Names of Faculty Supported

NAME	PERCENT_SUPPORTED	National Academy Member
Joshua L. Heitman	0.04	
FTE Equivalent:	**0.04**	
Total Number:	**1**	

Names of Under Graduate students supported

NAME	PERCENT_SUPPORTED
FTE Equivalent:	
Total Number:	

Student Metrics

This section only applies to graduating undergraduates supported by this agreement in this reporting period

The number of undergraduates funded by this agreement who graduated during this period: 0.00

The number of undergraduates funded by this agreement who graduated during this period with a degree in science, mathematics, engineering, or technology fields:...... 0.00

The number of undergraduates funded by your agreement who graduated during this period and will continue to pursue a graduate or Ph.D. degree in science, mathematics, engineering, or technology fields:...... 0.00

Number of graduating undergraduates who achieved a 3.5 GPA to 4.0 (4.0 max scale):...... 0.00

Number of graduating undergraduates funded by a DoD funded Center of Excellence grant for Education, Research and Engineering:...... 0.00

The number of undergraduates funded by your agreement who graduated during this period and intend to work for the Department of Defense 0.00

The number of undergraduates funded by your agreement who graduated during this period and will receive scholarships or fellowships for further studies in science, mathematics, engineering or technology fields:...... 0.00

Names of Personnel receiving masters degrees

NAME
Total Number:

Names of personnel receiving PHDs

NAME
Total Number:

Names of other research staff

NAME	PERCENT_SUPPORTED
FTE Equivalent:	
Total Number:	

Sub Contractors (DD882)

Inventions (DD882)

Scientific Progress

See Attachment

Technology Transfer

STIR PROJECT:
TRANSIENT SOIL DENSITY IMPACTS LAND SURFACE CHARACTERISTICS AND CHARACTERIZATION

Y. Kojima, J.L. Heitman (PI), and R. Horton

ABSTRACT
Soil density is commonly treated as static in studies on land surface property dynamics. Magnitudes of errors associated with this assumption are largely unknown. Objectives of this preliminary investigation were to: i) quantify effects of soil density variation on soil properties, and ii) evaluate impact of changing soil density on surface energy balance and heat and water transfer. Six soil properties were evaluated over a range of soil densities, using a combination of ten modeling approaches. Thermal conductivity, water characteristics, hydraulic conductivity, and vapor diffusivity were most sensitive; these properties changed by fractions greater than associated change in density (i.e., 10% change in density led to >10% change in property). Subsequently, three field seasons were simulated with a numerical model (HYDRUS-1D) for a range of bulk densities. Among the surface energy balance terms, ground heat flux and latent heat flux were most sensitive to bulk density. Surface soil temperature variation increased in with low bulk densities but subsurface temperature variation decreased. Surface water content varied with bulk density but effects mostly disappeared in the subsurface. Results demonstrate significance of transient density on surface conditions and point to need for continued evaluation of impacts with improved measurements and modeling.

INTRODUCTION

Surface soil is a complex, dynamic interface which dictates mass and energy transfer between land and atmosphere, and determines water flow and partitioning in the hydrological cycle. Its properties are considered dynamic because they are controlled in part by soil water content, which can change quickly with wetting events or slowly over sustained periods of drainage, plant uptake, and evaporative drying. Filling and emptying of water in soil pore space alters soil hydraulic and thermal properties. Because understanding soil-water controlled properties is critical for modeling and interpreting broader hydrologic and environmental processes, tremendous effort has been expended to develop soil water sensor technologies and monitoring networks (Robinson et al., 2008; Ochsner et al., 2013). This work has led to new understanding of soil property dynamics, and for potentially even greater understanding, as these measurements are coupled with remote sensing to extend measurement footprints (Albergel et al., 2012). Yet, in all of these efforts there remain fundamental questions that have not been addressed. An elementary and ubiquitous assumption in hydrologic studies considering dynamic soil surface properties is that soil density is static. We know, in fact, that this is not the case.

Consequences associated with this assumption are largely unknown, but are likely critical (cf. Arya and Paris, 1981; Moldrup et al., 2000; Ochsner et al., 2001). Large areas of the land surface undergo significant changes in surface soil density through annual cycles of disturbance associated with agriculture (Strudley et al., 2008; Logsdon, 2012; Liu et al., 2014). Freeze-thaw processes alter surface density and arrangement seasonally (Staricka and Benoit, 1995). Shrink-swell processes, erosion, and deposition alter surface soil density and arrangement episodically (Timm et al., 2006). Unfortunately, due to historical, practical limitations in our ability to continuously quantify soil density-derived effects, this limitation remains mostly unaddressed as a dynamic factor in land surface characterization, and the magnitudes of any associated errors are unknown to scientists and engineers working on a multitude of related investigations.

Our general goal is to examine the impact of transient (i.e., dynamic) soil density on land surface characteristics and characterization. Moving forward toward this goal likely requires both extensive measurement and modeling efforts. The objectives for this STIR project were focused toward making initial progress in work aimed at this longer-term goal.

Specific objectives for this project were to:

1) Quantify effects of soil density variation on fundamental soil properties.
2) Evaluate impact of changing soil density and associated properties on surface energy balance and coupled heat and water transfer in soils.

We first modeled a series of germane soil properties: volumetric heat capacity, thermal conductivity, soil thermal diffusivity, water retention characteristics, hydraulic conductivity, and vapor diffusivity using soil property models from the literature that included the capacity to incorporate bulk density dependence. We then used a subset of these properties in a numerical model to examine expected variation in surface energy balance terms, soil water content, and soil temperature associated with bulk density variation as a case study. In the following, methods and results are summarized together by analysis. Detailed interpretation is currently being pursued for a forthcoming manuscript.

PROPERTY MODELING (Objective 1)

We based our analysis on the range of bulk densities (ρ_b) observed in several previous field studies. Berndt and Coughlam (1976) investigated ρ_b changes associated with shrink-swell of a clay soil and reported values ranging from 1.04 to 1.37 Mg m^{-3} (32% variation) with wetting-drying cycles. Kays et al. (1985) showed, for a clay loam soil, that ρ_b change associated with freeze-thaw cycles was from 1.28 to 1.18 Mg m^{-3} (8% variation). Logsdon (2012) observed ρ_b variation, through periodic sampling over 5 yr in a clay loam, of 1.25 to 1.40 Mg m^{-3} (12% variation). Liu et al. (2014) observed ρ_b variations due to settling after tillage and reported values for silt loam changing from 1.00 to 1.35 Mg m^{-3} (35% change), and values for a sandy loam changed from 1.10 to 1.35 Mg m^{-3} (23% change).

We tested three soils in our analysis (Table 1): silt loam and sandy loam with data from Liu et al. (2014), and clay loam from Logsdon et al. (2012) using properties of a Webster soil series.

Soil Thermal Properties

Impact of ρ_b on soil ***volumetric heat capacity*** *C* was evaluated with the de Vries (1963) model,

$$C = c_s \rho_b + C_L \theta \qquad [1]$$

where c_s is specific heat of soil solid (J kg^{-1} °C^{-1}), C_L is volumetric heat capacity of liquid water (4,184,000 J m^{-3} K^{-1}) and θ is volumetric water content (m^3 m^{-3}). The values for c_s were calculated based on particle size distribution and soil organic matter content (SOM) as described by de Vries (1963). The *C* values were calculated for θ = 0.10 m^3 m^{-3} to 0.40 m^3 m^{-3} and with ρ_b = 1.10 Mg m^{-3} to 1.40 Mg m^{-3}.

As would be expected from the model, increasing ρ_b resulted in an increase of *C*, and the rate of increase was constant over the range of θ (Fig. 1). If we treat our minimum ρ_b as the standard and use θ = 0.25 m^3 m^{-3} for evaluation, a 100 kg m^{-3} increase in ρ_b results in 77-84 kJ m^{-3} K^{-1} increase in *C*. In percent, approximately 8% increase in ρ_b resulted in 4.0, 4.1, and 4.0 % increase in *C* for clay loam, silt loam, and sandy loam, respectively. The *C* values for observed maximum ρ_b were 106%, 110%, and 108% of the values for observed minimum ρ_b for clay loam, silt loam, and sandy loam, respectively.

Impact of ρ_b on soil ***thermal conductivity*** λ was evaluated with the de Vries (1963), Campbell (1985), and Lu et al. (2014) models. de Vries (1963) provided an equation to calculate λ based on the soil particle size distribution, ρ_b, and soil organic matter content:

$$\lambda = \frac{\sum_{i=0}^{N} k_i x_i \lambda_i}{\sum_{i=0}^{N} k_i x_i} \qquad [2]$$

where *N* is the number of types of soil constituents, k_i is a weighting factor, x_i is volume fraction, and λ_i is thermal conductivity of each soil constituent. Empirically determined values for k_i were used in this study.

Campbell (1985) provided the following equation

$$\lambda = A + B\theta - (A - D)\exp\left[-(E\theta)^4\right] \qquad [3]$$

where *A*, *B*, *D*, and *E* are shape factors associated with soil properties. Empirical parameters can be calculated as:

$$A = \frac{0.57 + 1.73\theta_q + 0.93\theta_m}{1 - 0.74\theta_q - 0.49\theta_m} - 2.8\theta_{solid}(1 - \theta_{solid}) \qquad [4]$$

$$B = 2.8\theta_{solid} \qquad [5]$$

$$D = 0.03 + 0.7\theta_{solid} \qquad [6]$$

$$E = 1 + 2.6 m_c^{-0.5} \qquad [7]$$

where θ_q is volume fraction of quartz, θ_m is volume fraction of other minerals, θ_{solid} is volume fraction of soil solid, and m_c is clay fraction. This model does not account for soil organic matter. In this study we assumed that θ_q is equal to volume fraction of sand, and θ_m is equal to the volume fraction of silt plus clay.

Lu et al. (2014) provided the following equation

$$\lambda = \lambda_{dry} + \exp\left(\beta - \theta^{-\alpha}\right) \qquad [8]$$

where λ_{dry} is thermal conductivity of oven dried soil, and α and β are shape factors. The thermal conductivity of oven dried soil can be estimated from soil porosity τ.

$$\lambda_{dry} = -0.56\tau + 0.51 \qquad [9]$$

The shape factors α and β can be determined based on soil particle distribution and ρ_b

$$\alpha = 0.67 f_{cl} + 0.24 \qquad [10]$$

$$\beta = 1.97 f_{sa} + 0.00187\rho_b - 0.00136 f_{sa}\rho_b - 0.95 \qquad [11]$$

where f_{cl} is clay mass fraction, f_{sa} is sand mass fraction.

For the de Vries (1963) model, λ increases with increases of ρ_b and θ (Fig. 2). Values of λ were highest for sandy loam, and lowest for silt loam (sandy loam>clay loam> silt loam). When θ = 0.25 m^3 m^{-3}, a 100 kg m^{-3} (8%) increase in ρ_b results in 12.8%, 11.9%, and 14.4% increases in λ for clay loam, silt loam, and sandy loam, respectively. The λ values for observed maximum ρ_b were 122%, 140%, and 131% of the values for observed minimum ρ_b for clay loam, silt loam, and sandy loam, respectively.

The Campbell (1985) model is shown in Fig. 3. Trends were similar to those from the de Vries (1963) model, but values of λ were generally larger. Values of λ were highest for sandy loam, and lowest for silt loam (sandy loam>silt loam> clay loam). With θ = 0.25 m^3 m^{-3}, a 100 kg m^{-3} increase in ρ_b caused 11.2%, 11.0%, and 11.8% increases of λ for clay loam, silt loam, and sandy loam, respectively. The λ values for observed maximum ρ_b were 117%, 130%, and 125% of the values for observed minimum ρ_b for clay loam, silt loam, and sandy loam, respectively. These percentage increases are smaller than those with the de Vries model, despite similar changes in λ, because of generally higher λ values for the Campbell model.

The Lu et al. (2014) model followed similar trends as the other models (Fig. 4). With θ = 0.25 m^3 m^{-3}, a 100 kg m^{-3} increase in ρ_b caused 15.4%, 16.4%, and 12.0% increases in λ for clay loam, silt loam, and sandy loam, respectively. The λ values for observed maximum ρ_b were 124%, 146%, and 125% of the values for observed minimum ρ_b for clay loam, silt loam, and sandy loam, respectively.

Thermal diffusivity κ (=λ/C) was calculated as a function of ρ_b and θ based on the de Vries (1963) model for C and Campbell (1985) model for λ (Fig. 5). The effect of ρ_b is very small with $\theta < 0.15$ m^3 m^{-3} for clay loam and silt loam, but generally increases in ρ_b resulted in increases in κ. With $\theta = 0.25$ m^3 m^{-3}, a 100 kg m^{-3} increase in ρ_b caused 7.0%, 6.6%, and 7.5% increases in κ for clay loam, silt loam, and sandy loam, respectively. The κ values for observed maximum ρ_b were 111%, 118%, and 116% of values for observed minimum ρ_b for clay loam, silt loam, and sandy loam, respectively.

Soil Hydraulic Properties

Water characteristics were first examined at different values of ρ_b and θ using ROSETTA, which is a hierarchical pedotransfer function (Schaap et al., 2001). Empirical parameters for the van Genuchten (1980) water retention model: θ_s, θ_r, α, and n are output by ROSETTA. ROSETTA also outputs saturated hydraulic conductivity K_s. The van Genuchten (1980) model is

$$\theta = \theta_r + (\theta_s - \theta_r)\left[\frac{1}{1+|\alpha\psi|^n}\right]^{1-1/n} \qquad [12]$$

where ψ (m) is soil water matric potential, θ_s and and θ_r are often referred to as saturated and residual water contents, respectively.

Increases in ρ_b caused decreases in θ_r, θ_s, and K_s (Table 2). Decreases in θ_s and K_s are reasonable but values for θ_r are expected to increase because of reduction of pore size (Assouline, 2006a). Figure 6 shows resulting soil water retention curves as a function of ρ_b and ψ. Increases in ρ_b shift the water retention curves downward. A significant impact of ρ_b increase is shown clearly in the decrease of saturated water contents. There are also relatively large differences in matric potential when soil is dry. With ψ = -10 m, water content decreased 0.002-0.008 m^3 m^{-3} for a 100 kg m^{-3} increase in ρ_b. Impact of altering ρ_b is more significant in finer textured soil, i.e., clay loam.

The effect of ρ_b changes on water characteristics was also tested with the model suggested by Assouline (2006a). Assouline (2006a) described the water retention curve as

$$S_e = 1 - \exp\left\{-\left[\alpha\left(|\psi|^{-1} - |\psi_L|^{-1}\right)\right]^{\mu}\right\} \qquad [13]$$

where S_e is degree of saturation, $S_e = (\theta-\theta_r)/(\theta_s-\theta_r)$, α and μ are fitting parameters, ψ_L is matric potential corresponding to a very small water content, θ_L, which represents the limit of the domain of interest of the water retention curve. For convenience, θ_r can be assumed to equal θ_L.

Brooks and Corey (1964) suggested the following expression of the water retention curve

$$\begin{aligned} S_e &= (\psi/\psi_a)^{-\sigma} & \psi &< \psi_a \\ S_e &= 1 & \psi &\geq \psi_a \end{aligned} \qquad [14]$$

where ψ_a is air entry pressure, and σ is a pore-size distribution index. Assouline showed that σ is related to parameters in Eq. [13]

$$\sigma = 0.81\varepsilon^{-0.837} \qquad [15]$$

$$\varepsilon = \frac{(\alpha^{\mu})^{-1/\mu}\Gamma(1+1/\mu)+1/|\psi_L|}{\left\{(\alpha^{\mu})^{-2/\mu}\left[\Gamma(1+2/\mu)-\Gamma^2(1+1/\mu)\right]\right\}^{1/2}} \quad [16]$$

Assouline (2006a) presented equations where water retention curves at varying ρ_b can be estimated when fitting parameters α, μ, and ψ_a are determined with experimental data at one ρ_b. The parameters in Eqs. [13]-[14] for the new water retention curve with different ρ_b, α_c, μ_c, and ψ_{ac}, are described as

$$\alpha_c = \alpha(\rho_{bc}/\rho_b)^{3.72} \quad [17]$$

$$\mu_c = \mu(\rho_{bc}/\rho_b)^{\omega} \quad [18]$$

$$\psi_{ac} = \psi_a(\rho_{bc}/\rho_b)^{3.82} \quad [19]$$

where ρ_b and ρ_{bc} are original and new bulk densities, and ω is defined as

$$\omega = 2.3 - 1.9(SC/CC)^{-0.5} \quad [20]$$

where SC and CC are mass fraction of silt and clay. The values for θ_s and θ_r also change with changes in ρ_b. Assouline (2006a) presented

$$\theta_{sc} = \theta_s\left[(\rho_s - \rho_{bc})/(\rho_s - \rho_b)\right] \quad [21]$$

$$\theta_{rc} = \theta_r(\rho_{bc}/\rho_b) \quad [22]$$

where θ_{sc} are θ_{rc} are saturated and residual water content with the new ρ_b value, and ρ_s is soil solid density (≈2650 kg m^{-3}).

In this study, we first obtained water retention parameters for the van Genuchten (1980) model from ROSETTA for clay loam, silt loam, and sandy loam at ρ_b = 1.25 Mg m^{-3}. Parameters for Eqs. [13]-[14] were determined by fitting data from these water retention curves. Based on these parameters and new ρ_b, water retention curves were estimated with Eqs. [15]-[21].

Table 3 shows a subset of the parameters required for Eqs. [12]-[14] at different ρ_b. Estimates of θ_r were plausible by this approach in that θ_r decreases as ρ_b decreases. Thus, the water retention curves with different ρ_b values cross one another (Fig. 7). At the same ψ, water content sometimes increased and sometimes decreased, depending on ψ and soil type. For example, when ψ = -1 m and with a 100 kg m^{-3} increase in ρ_b, water content increased 0.02 in clay loam, water content decreased 0.03 in silt loam, and water content increased 0.01-0.02 in sandy loam. When ψ = -10 m and with a 100 kg m^{-3} increase in ρ_b, water content increased 0.004 in clay loam, water content decreased 0.004 in silt loam, and water content decreased 0.01 in sandy loam.

Hydraulic conductivity *K* can be expressed by the van Genuchten model (1980) and parameters provided by ROSETTA as

$$K(S_e) = K_s S_e^{0.5}\left[1-\left(1-S_e^{1/m}\right)^m\right]^2 \quad [23]$$

where S_e for Eq. [23] is

$$S_e = \left[\frac{1}{1+|\alpha\psi|^n}\right]^{1-1/n} \qquad [24]$$

Hydraulic conductivity as a function of ψ and ρ_b is shown in Fig 8 (and K_s is given in Table 2). As would be expected, K consistently decreased with increasing ρ_b.

Assouline (2006b) presented an alternate model to describe K_s as a function of ρ_b, the value K_{sc} is

$$K_{sc} = K_s\left(\frac{\theta_{sc}-\theta_{rc}}{\theta_s-\theta_r}\right)^{2.5}\left(\frac{\psi_a}{\psi_{ac}}\right)^2\left[\frac{\sigma_c(1+\sigma)}{\sigma(1+\sigma_c)}\right]^2 \qquad [25]$$

where K_s, θs, θ_r, ψ_a, and σ are saturated hydraulic conductivity, saturated water content, residual water content, air entry pressure, and pore size distribution index at standard ρ_b, and θ_{sc}, θ_{rc}, ψ_{ac}, and σ_c are saturated water content, residual water content, air entry pressure, and pore size distribution index at the new ρ_b. Unsaturated hydraulic conductivity $K(S_e)$ for a variety of ρ_b were estimated with the Mualem (1976) and Brooks and Corey (1964) model

$$K(S_e) = K_s S_e^{(2+2.5\sigma)/\sigma} \qquad [26]$$

Values of K_s for different ρ_b are shown in Table 3. Note that K_s at 1.25 Mg m^{-3} was used as the standard for modification at other ρ_b according to Eq. [26]. Figure 9 shows K estimated with Eqs. [25] and [26] as a function of ρ_b and ψ instead of S_e. Relative effects -- K decreases with increasing ρ_b -- are similar to those obtained from ROSETTA, despite differences in the water characteristics discussed earlier because the Mualem model treats residual water content as immobile.

Vapor diffusivity D_v in soil can be described as (Saito et al., 2006)

$$D_v = \tau\,\theta_a D_a \qquad [27]$$

where τ is a tortuosity factor, θ_a is air filled porosity, and D_a is water vapor diffusivity in air. The tortuosity factor can be described as (Millington and Quirk, 1961)

$$\tau = \frac{\theta_a^{7/3}}{\theta_s^{2}} \qquad [28]$$

Since θ_a and θ_s are simple functions of ρ_b and soil water content, there is no influence of different soil type on D_v. Values for D_v decrease with increasing ρ_b because of the associated decrease in θ_a (Fig. 10). When θ is 0.25 m^3 m^{-3}, a 100 kg m^{-3} increase of ρ_b caused 28.6%, 23.3%, and 24.9% decrease in D_v for clay loam, silt loam, and sandy loam, respectively. The D_v values for observed maximum ρ_b were 58.8%, 47.2%, and 53.6% of the values for observed minimum ρ_b for clay loam, silt loam, and sandy loam, respectively.

Key Findings from Property Modeling

Six soil thermal and hydraulic properties were evaluated for three soil textures over a realistic range in transient field soil bulk density, using a combination of ten models/modeling approaches available from the literature. The properties that appeared to be most sensitive to bulk density are as follows:

- Thermal conductivity – change of <10% in bulk density led to 11-16% change in thermal conductivity.

- Water characteristics – 25% change in bulk density led to 20-25% change in residual and saturated water contents, with changes occurring in opposite directions (i.e., larger residual water content and smaller saturated water content).
- Saturated hydraulic conductivity – values for saturated hydraulic conductivity typically change by an order of magnitude over the range of transient field bulk density.
- Vapor diffusivity – change of <10% in bulk density led to 23-29% change in diffusivity.

NUMERICAL SIMULATIONS (Objective 2)

Simulations were performed with the HYDRUS-1D software package (Šimůnek et al., 2009) to evaluate impacts of change in bulk density on surface energy balance and soil heat and water transfer. Four soil profiles (A, B, C, and D) were used in the simulations, each approximately representing a soil with silt loam texture. The soil profiles have two layers (Fig. 11), one represents a disturbed soil layer (0-0.225 m depth) which has ρ_b = 1.3 (A), 1.2 (B), 1.4 (C) or 1.5 (D) Mg m^{-3} bulk density, and the other is an undisturbed deep soil layer (0.225-5 m depth) which has ρ_b = 1.4 Mg m^{-3}. (Thus, profile (C) has uniform ρ_b throughout the profile.) Node spacing was 0.01 m from surface through 50 cm depth, and node spacing was gradually increased to a maximum of 0.05 m below 50 cm depth. Hydraulic properties were expressed with the Brooks and Corey (1964) model, and parameters were obtained with the Assouline (2006a) approach described above. Thermal properties were calculated with the Campbell (1985) model.

Weather data from an experimental field near Ames, IA in 2012, 2013, and 2014 were used to determine surface boundary conditions. Calculations were made with data during May-October in each year. These three years provide differing amounts of precipitation during May-October. Accumulated precipitation in May-October was 337, 524, and 801 mm in 2012, 2013, and 2014, respectively, i.e., 2012 was a dry year, 2013 was intermediate, and 2014 was wet. Accumulated solar radiation during May-October was 3781, 3422, and 3216 MJ m^{-2} in 2012, 2013, and 2014, respectively. The dry year (2012) had greater accumulated solar energy.

The soil surface boundary condition was determined by the calculated surface energy balance and the observed precipitation. The calculation processes are described in Šimůnek et al. (2009). The bottom boundary conditions were free drainage for water transport and zero gradient for heat transport. The initial condition for water content was 0.25 m^3 m^{-3} for all depths and the initial condition for temperature was 20ºC at all depths.

Surface Energy Balance

Across all three years, ***Net radiation*** was smaller during the daytime and larger at night when ρ_b was low (not shown). The relatively small differences were likely associated with differences in surface albedo and longwave radiation from soil surface. ***Ground heat flux*** showed relatively large differences with ρ_b variation, particularly for dynamic fluxes within a given day (Fig. 12). Accumulated differences on an annual basis were relatively small (Table 4). In 2013 and 2014, ground heat flux was relatively small at ρ_b = 1.2 Mg m^{-3}, and generally increased with ρ_b (Table 4). This may be associated with greater thermal conductivity with larger ρ_b. However, trends differed in 2012 when conditions were driest. In most cases smaller ρ_b produced larger ***latent heat flux*** (not shown). Accumulated latent heat flux (calculated as evaporation depth) was the highest with the lowest ρ_b in each simulated year (Table 4). This trend likely corresponds with increased storage of water available for evaporation from changes to the water characteristics and with greater vapor diffusivity at low ρ_b. Based on these differences, surface energy partitioning shifted toward a relatively greater proportion of available energy partitioning to sensible heat flux when ρ_b was largest.

Soil Heat and Water Dynamics

Soil temperature at the 5 cm soil depth generally showed greatest daily variation with low ρ_b (Fig. 13). Differences in temperature at maximum and minimum were typically on the order of 1 °C with low ρ_b having both the largest maximum and smallest minimum (i.e., difference in variation of 2 °C). At the 30 cm soil depth, where ρ_b was the same for each simulated profile, surface ρ_b also influenced observed temperatures (Fig. 14). However, in this case the trend was opposite that observed at the surface. At the 30 cm depth, daily temperature variation increased with high surface ρ_b. In this case, the surface layer with low ρ_b, and thus low thermal conductivity, acts as insulation, muting temperature variation in the subsurface. On a seasonal basis, high surface ρ_b results in earlier warming in the summer and earlier cooling in the fall (Fig. 15).

Soil water content at the 5 cm depth was generally drier at low ρ_b (Fig. 16). This result is likely a combination of both more rapid drainage during rainfall events, and lower residual water content retained. During a typical drying event, simulated water content at low ρ_b was about 0.02 $m^3\ m^{-3}$ lower than at the largest ρ_b (Fig. 17). At the 30 cm depth, differences between profiles with different ρ_b were generally small (not shown).

Key Findings from Numerical Simulation

Three seasons with differing surface conditions (rainfall, solar radiation) were simulated with a numerical model for a range of bulk density conditions. Main findings were that as bulk density increased:

- Ground heat flux increased by as much as 25% on an annual basis, though effects varied by year.
- Evaporation rate (latent heat flux) decreased by as much as 7-8% on an annual basis.
- Surface layer temperature variation decreased – differences in variation at the 5 cm depth were on the order of 2 °C.
- Subsurface layer temperature variation increased – even at 30 cm depth, the effect was on the order of 1 °C.
- Surface soil water content increased by about 0.02 $m^3\ m^{-3}$ during typical drying events.

BIBLIOGRAPHY

Assouline, S. 2006a. Modeling the relationship between soil bulk density and the water retention curve. Vadose Zone J. 5:554-563.

Assouline, S. 2006b. Modeling the relationship between soil bulk density and the hydraulic conductivity function. Vadose Zone J. 5:697-705.

Berndt, R.D., and K.J. Coughlam. 1976. The nature of changes in bulk density with water content in a cracking clay. Aust. J. Soil Res. 15:27-37.

Brooks, R. H., and A. T. Corey. 1964. Hydraulic properties of porous media. Hydrology Paper No. 3. Fort Collins, Colo.: Colorado State University.

Campbell, G.S. 1985. Soil Physics with BASIC. Elsevier, New York

de Vries, D.A. 1963. Thermal properties of soils. In: W.R. van Wijk, editor, Physics of plant environment. 2nd ed. North Holland Publ., Amsterdam. p. 210-235.

Han, W., Y. Gong, T. Ren, and R. Horton. 2014. Accounting for time-variable soil porosity improves the accuracy of the gradient method for estimating soil carbon dioxide production. Soil Sci. Soc. Am. J. 78:1426-1433.

Kay, B.D., C.D. Grant, and P.H. Groenevelt. 1985. Significance of ground freezing on soil bulk density under zero tillage. Soil Sci. Soc. Am. J. 49:973-978.

Liu, X., S. Lu, R. Horton, and T. Ren. 2014. In situ monitoring of soil bulk density with a thermo-TDR sensor. Soil Sci. Soc. Am. J. 78:400-407.

Logsdon, S.D. 2012. Temporal variability of bulk density and soil water at selected field sites. Soil Sci. 177:327-331.

Lu, Y., S. Lu, R. Horton, and T. Ren. 2014. An empirical model for estimating soil thermal conductivity from texture, water content, and bulk density. Soil Sci. Soc. Am. J. 78:1859-1868.

Ma, L., L.R. Ahuja, B.T. Nolan, R.W. Malone, T.J. Trout, and Z. Qi. 2012. Root zone water quality model (RZWQM2): model use, calibration, and validation. Trans. ASABE 55:1425-1446.

Millington, R.J., and J.P. Quirk. 1961. Permeability of porous media. Trans. Faraday Soc.57:1200-1207.

Moldrup, P., T. Olesen, J. Gamst, P. Schjønning, T. Yamaguchi and D.E. Rolston. 2000. Predicting the gas diffusion coefficient in repacked soil water-induced linear reduction model. Soil Sci. Soc. Am. J. 64:1588-1594.

Mualem, Y. 1976. A new model for predicting the hydraulic conductivity of unsaturated porous media. Water Resour. Res. 12:513-522.

Schaap, M.G., F.J. Leij, and M. Th. van Genuchten. 2001. ROSETTA: a computer program for estimating soil hydraulic parameters with hierarchical pedotransfer functions. J. Hydrol. 251:163-176.

Šimůnek, J., M. Šejna, H. Saito, M. Sakai, and M. Th. van Genuchten. 2009. The HYDRUS-1D software package for simulating the one-dimensional movement of water, heat, and multiple solutes in variably saturated media. Version 4.08. http://www.pc-progress.com/Downloads/Pgm_hydrus1D/HYDRUS1D-4.08.pdf

van Genuchten, M.Th. 1980. A closed-form equation for predicting the hydraulic conductivity of unsaturated soils. Soil Sci. Soc. Am. J. 44:892-898.

Wösten, J.H.M., A. Lilly, A. Nemes, and C. Le Bas. 1999. Development and use of a database of hydraulic properties of European soils. Geoderma 90:169-185.

Table 1. Soil particle size distribution, soil organic matter content (SOM), and observed minimum and maximum values for soil bulk density.

	Particle size distribution				Bulk density	
Texture	Sand	Silt	Clay	SOM	Min	Max
				kg kg^{-1}	kg m^{-3}	
Clay loam	21	47	32	0.07	1250	1400
Silt loam	17	62	21	0.01	1100	1350
Sandy loam	53	38	9	0.01	1150	1350

Table 2. Empirical parameters for the van Genuchten (1980) model output with ROSETTA (Schaap et al., 2001) as a function of soil bulk density.

Parameter	Bulk density		
	Mg m^{-3}		
	1.1	1.25	1.4
		Clay loam	
θ_r	0.091	0.088	0.084
θ_s	0.522	0.480	0.441
K_s (cm d^{-1})	53.2	22.5	9.6
		Silt loam	
θ_r	0.078	0.074	0.071
θ_s	0.495	0.455	0.419
K_s (cm d^{-1})	70.5	33.7	15.8
		Sandy loam	
θ_r	0.045	0.042	0.040
θ_s	0.442	0.432	0.377
K_s (cm d^{-1})	121	68.8	40.1

Table 3. Empirical parameters for the Assouline (2006) approach as a function of soil bulk density. Parameters at bulk density = 1.25 Mg m-3 were estimated with ROSETTA (Schaap et al., 2001).

Parameter	Bulk density		
	Mg m^{-3}		
	1.1	1.25	1.4
	Clay loam		
θ_r	0.080	0.088	0.102
θ_s	0.531	0.480	0.428
ψ_a (cm)	52.2	85.0	131
σ	0.47	0.52	0.57
K_s (cm d^{-1})	76.1	22.5	6.82
	Silt loam		
θ_r	0.067	0.074	0.085
θ_s	0.504	0.455	0.406
ψ_a (cm)	90.3	147	227
σ	0.546	0.63	0.72
K_s (cm d^{-1})	106	33.7	10.8
	Sandy loam		
θ_r	0.040	0.042	0.051
θ_s	0.452	0.408	0.365
ψ_a (cm)	40.4	65.8	102
σ	0.42	0.51	0.59
K_s (cm d^{-1})	193	68.8	24.6

Table 4. Accumulated ground heat flux (positive downward) and evaporation as a function of soil bulk density for May to October in each simulation year.

	Soil bulk density (surface)			
	Mg m^{-3}			
	1.1	1.3	1.4	1.5
Year	Cumulative ground heat flux			
	MJ m^{-2}			
2012	13.4	13.3	13.1	13.2
2013	6.0	5.7	6.1	6.4
2014	-4.6	-4.1	-3.7	-3.6
	Cumulative evaporation			
	mm			
2012	390	380	371	363
2013	576	569	563	557
2014	858	854	852	849

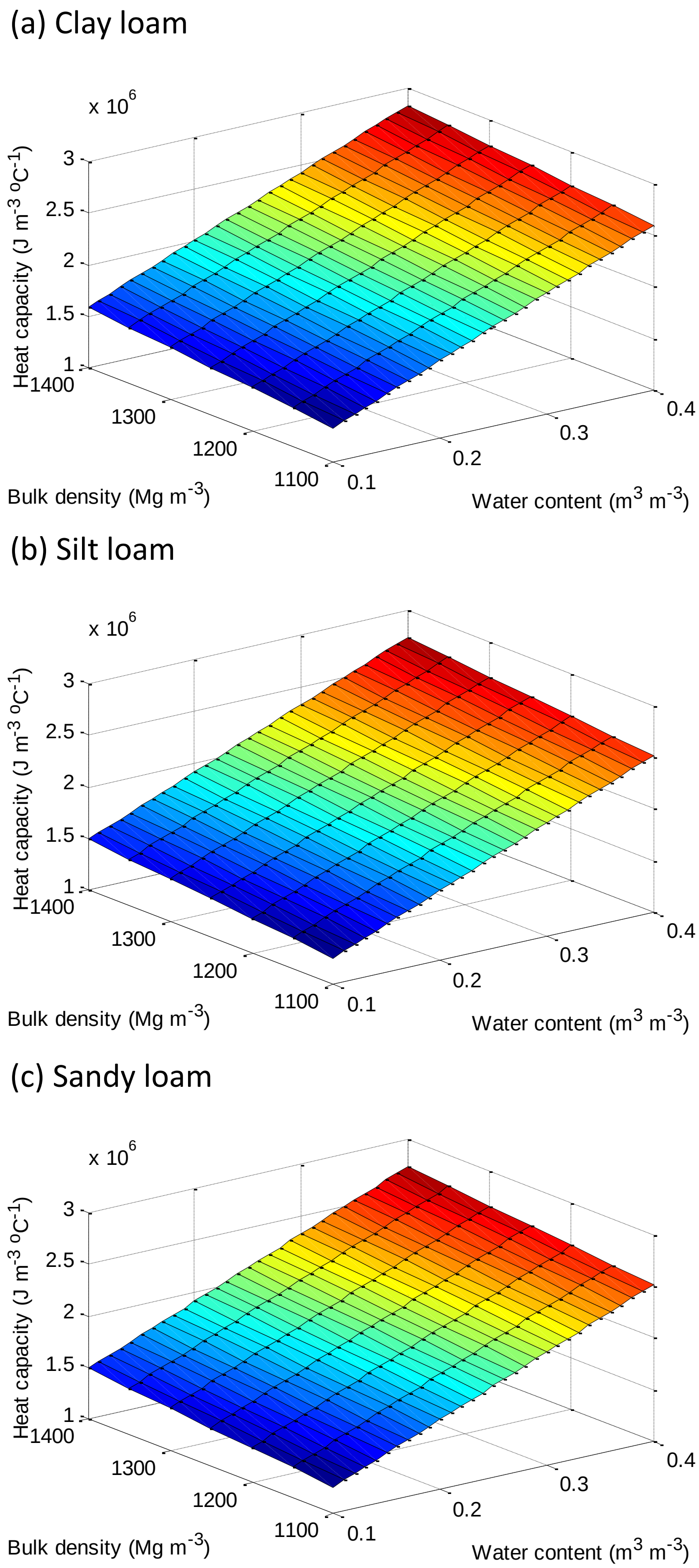

Figure 1. Volumetric heat capacity as a function of bulk density and volumetric water content.

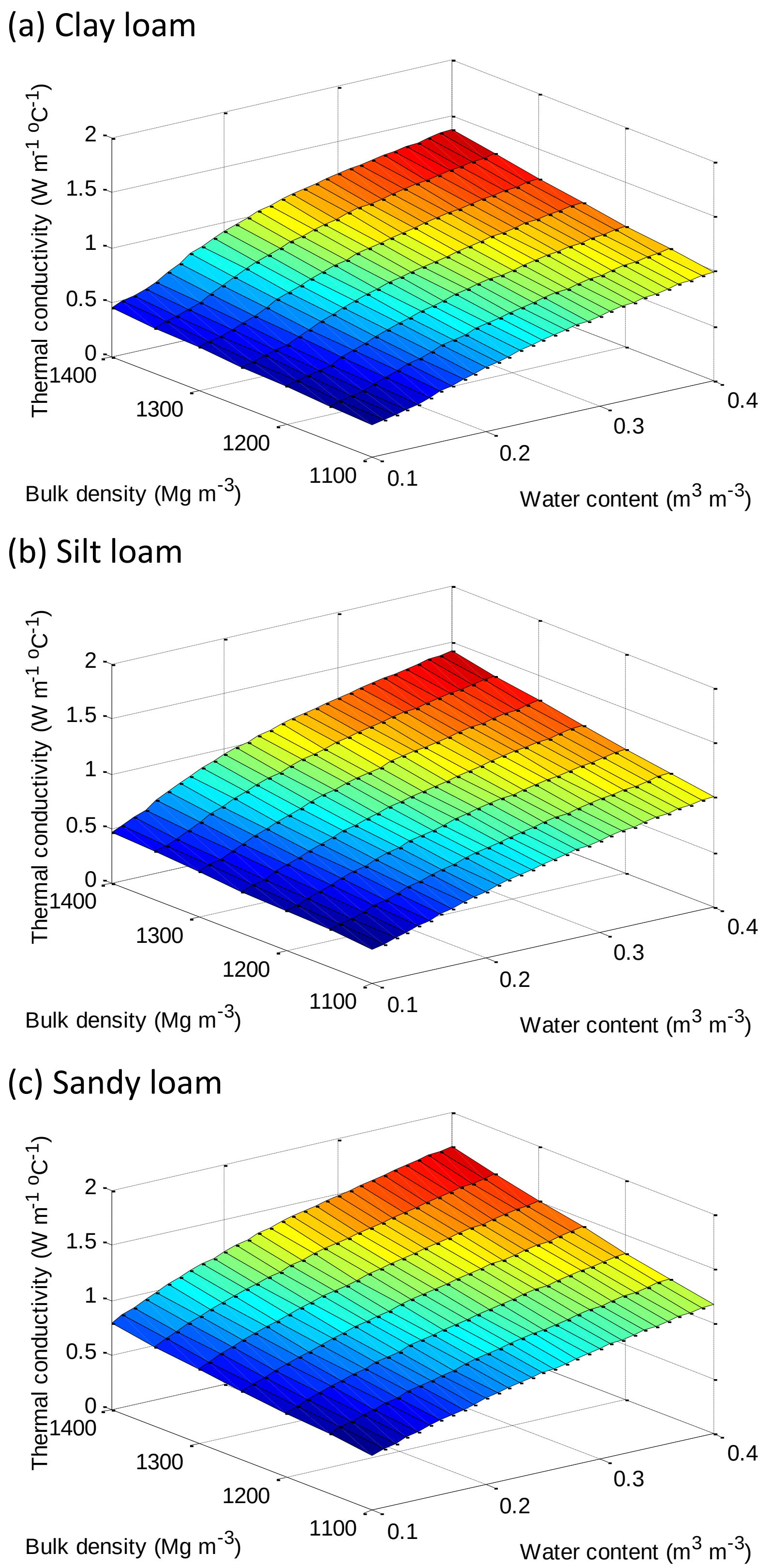

Figure 2. Thermal conductivity as a function of bulk density and volumetric water content with de Vies (1963) model.

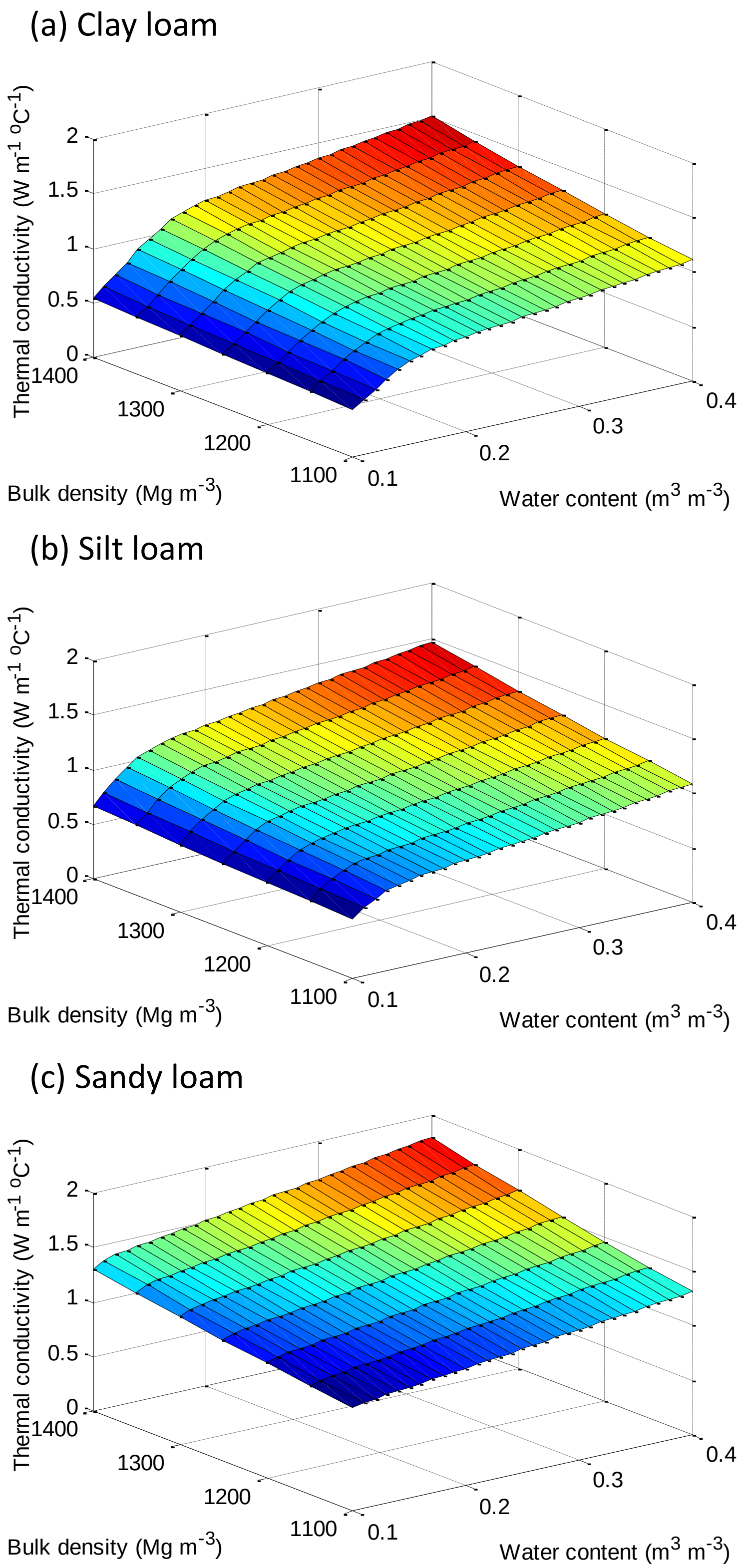

Figure. 3. Thermal conductivity as a function of bulk density and volumetric water content with Campbell (1985) model.

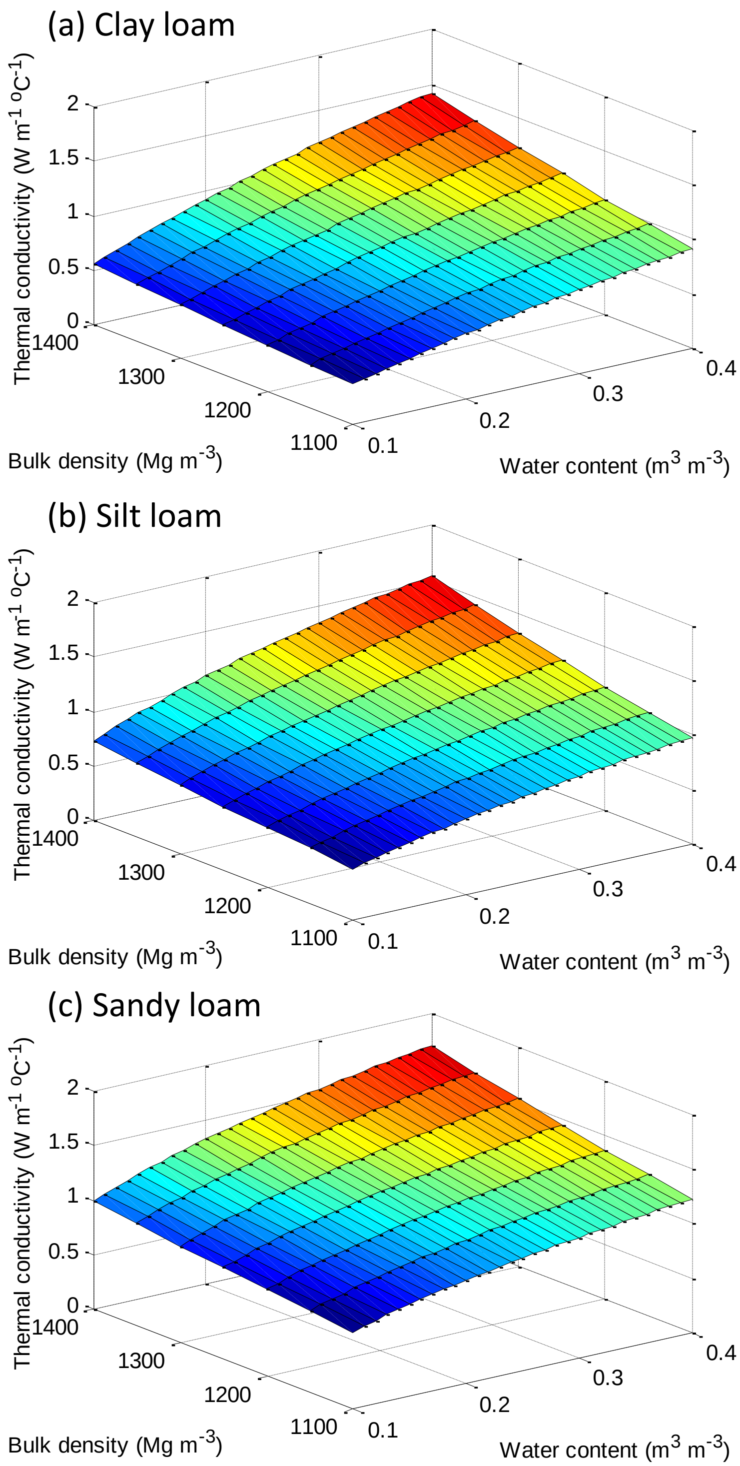

Figure 4. Thermal conductivity as a function of bulk density and volumetric water content with Lu et al. (2014) model.

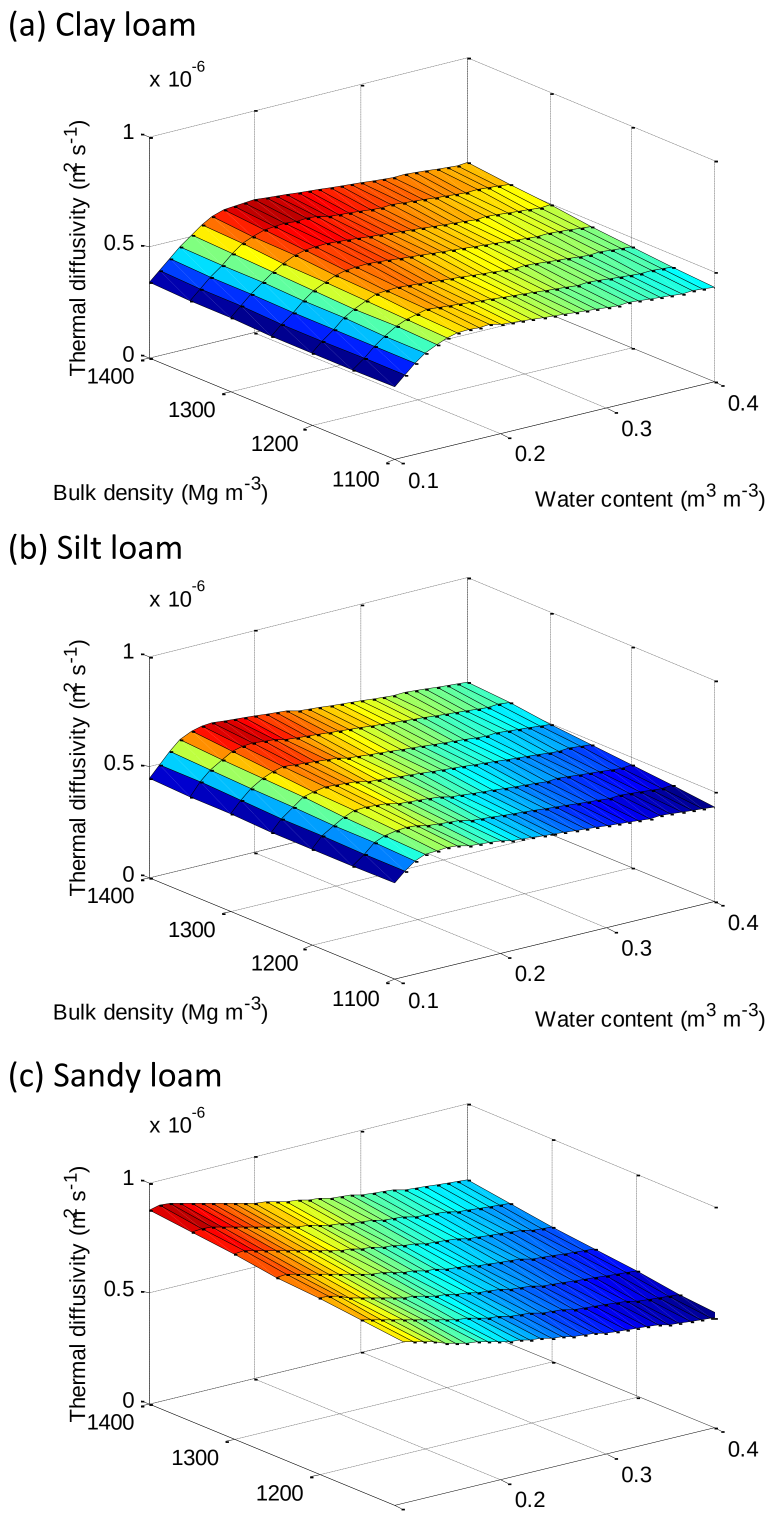

Figure 5. Thermal diffusivity as a function of bulk density and volumetric water content based on thermal conductivity determined with Campbell (1985) model and heat capacity determined with the de Vries (1963) model.

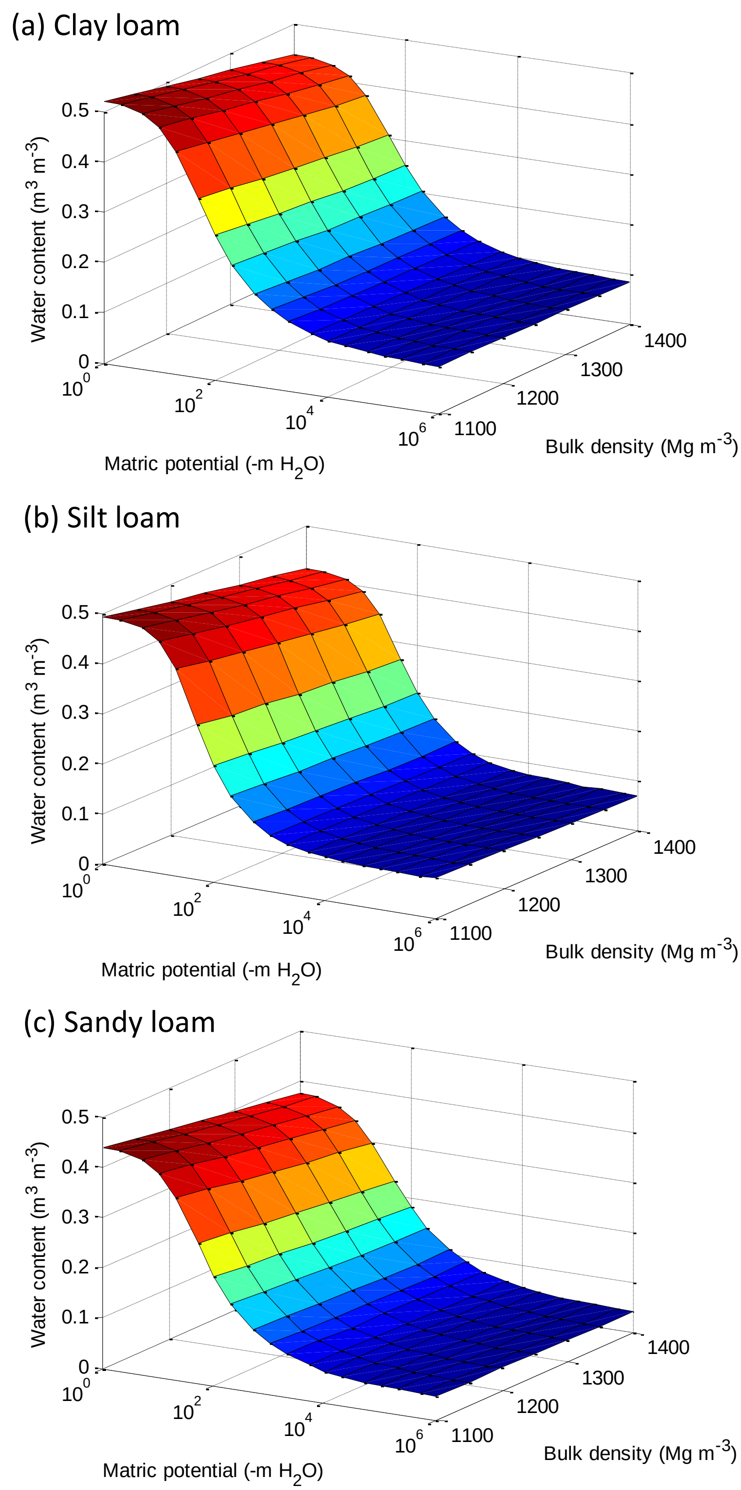

Figure 6. Water characteristics estimated with ROSETTA (Schaap et al., 2001) for different values of soil bulk density.

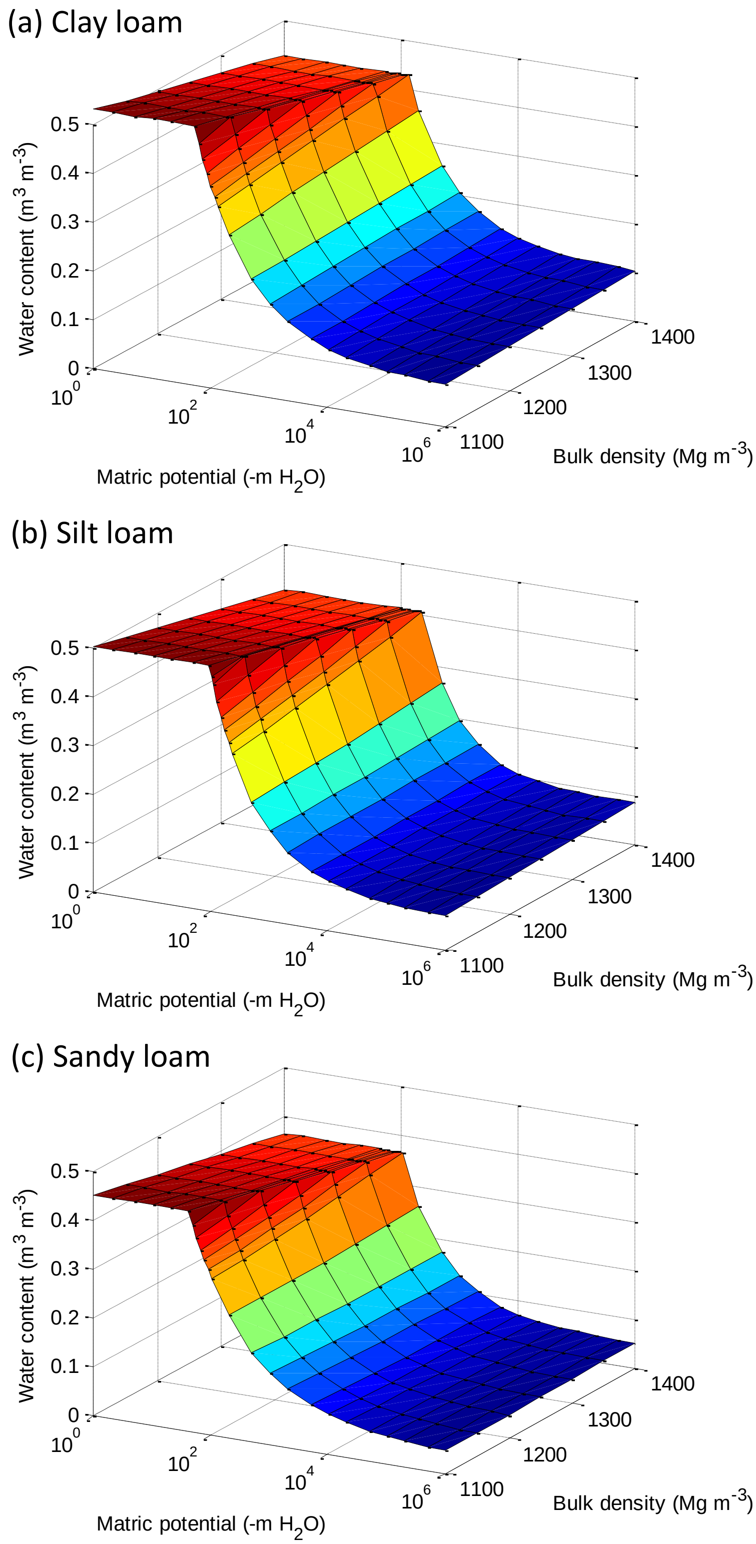

Figure 7. Water characteristics estimated with Assouline (2006a) and Brooks and Corey (1964) models at different values for bulk density.

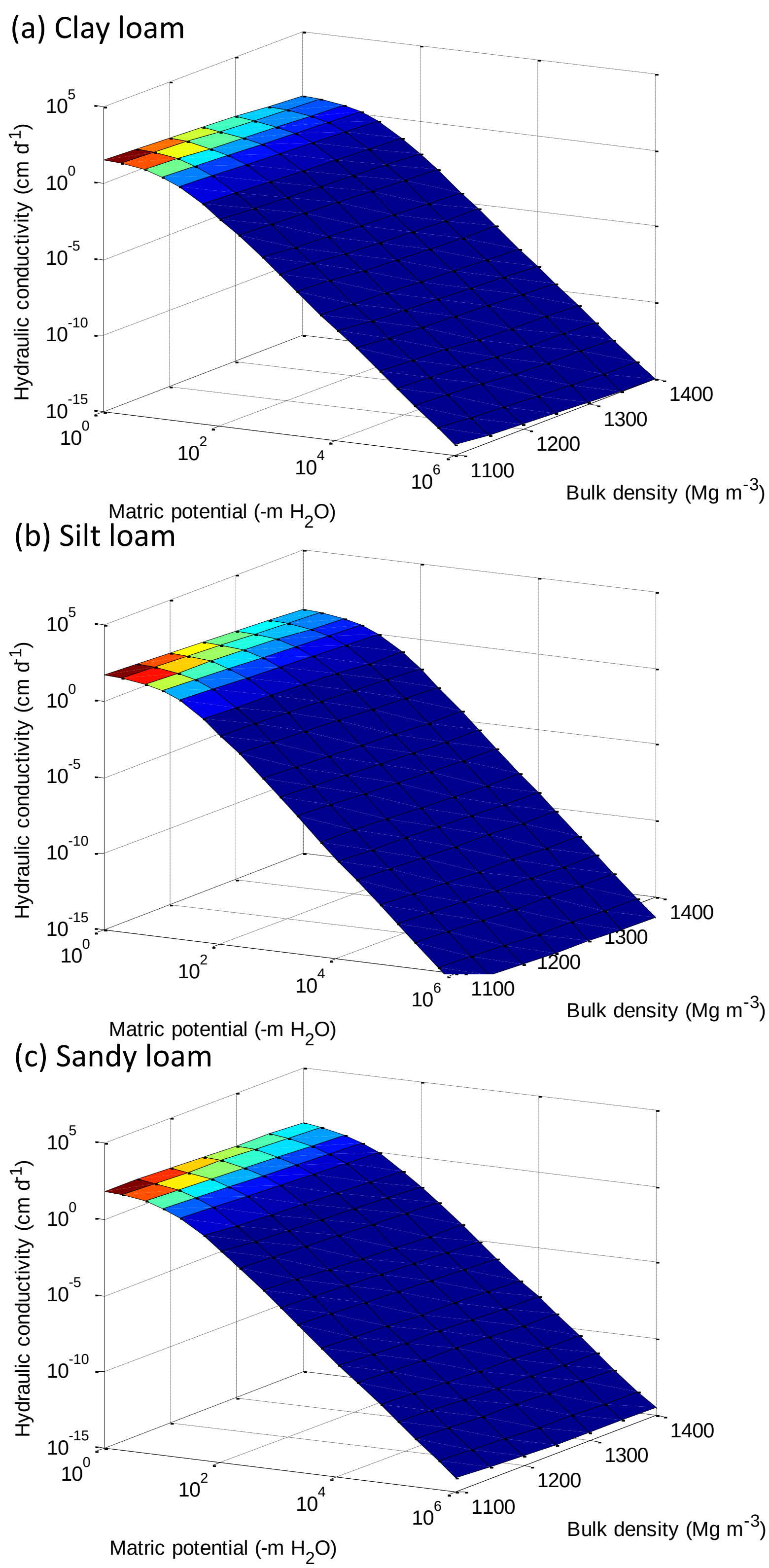

Figure 8. Hydraulic conductivity estimated with ROSETTA for different values of bulk density.

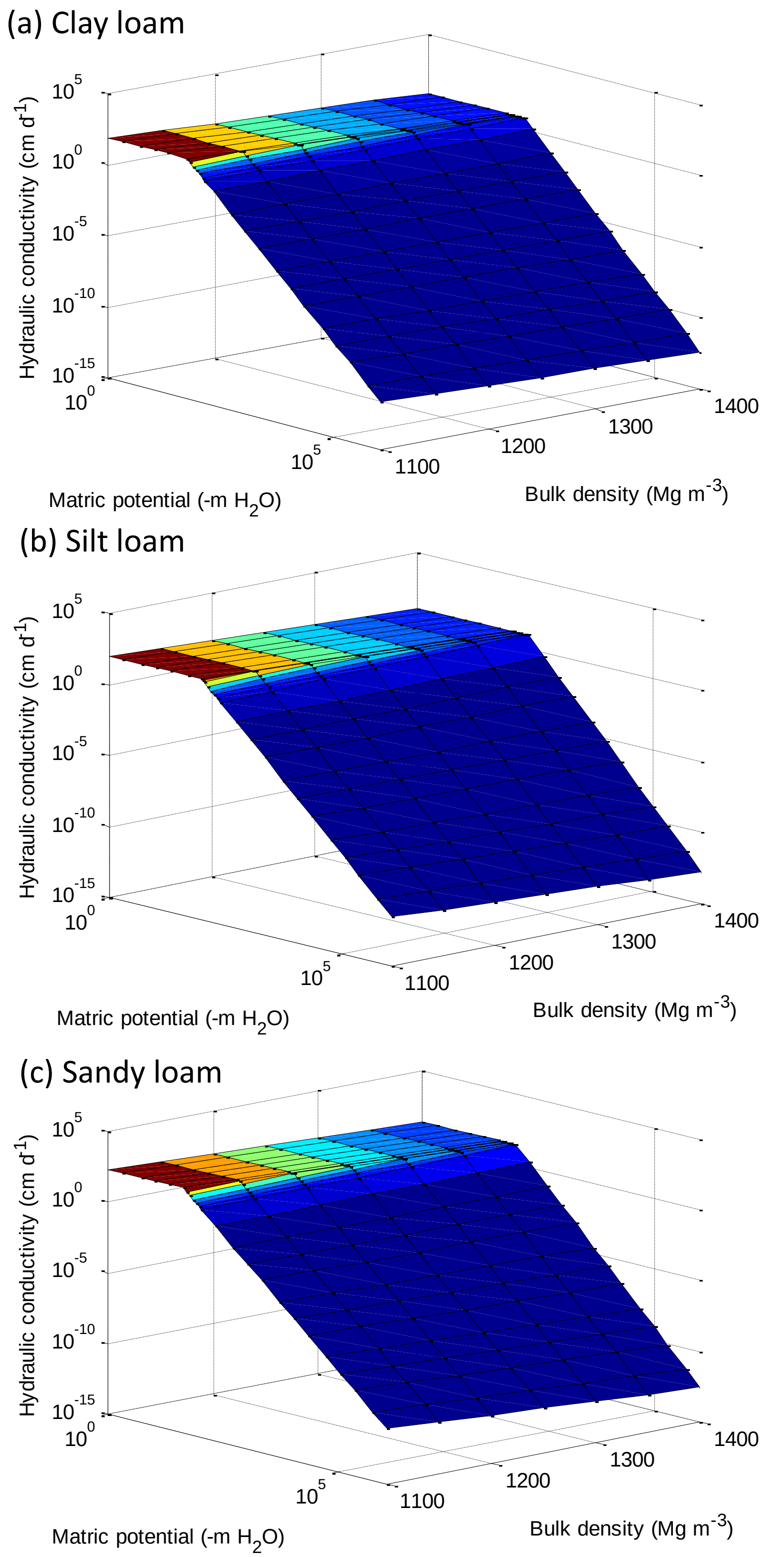

Figure 9. Hydraulic conductivity with Mualem (1976) and Brooks and Corey (1964) models with different values for bulk density.

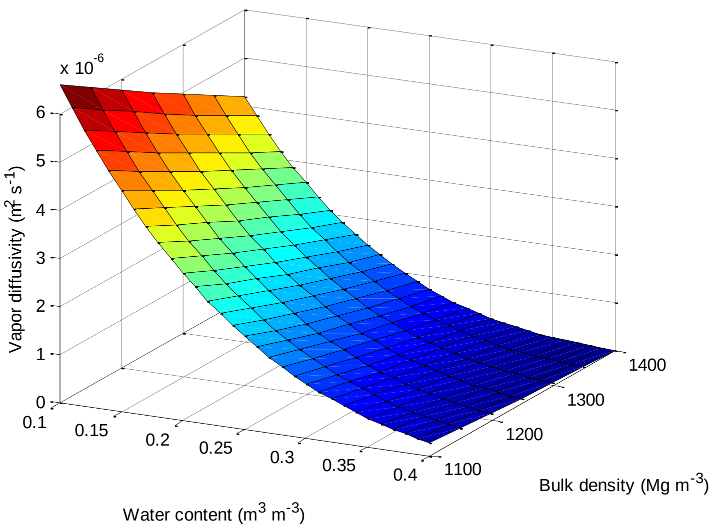

Figure 10. Vapor diffusivity in soil with different values for bulk density.

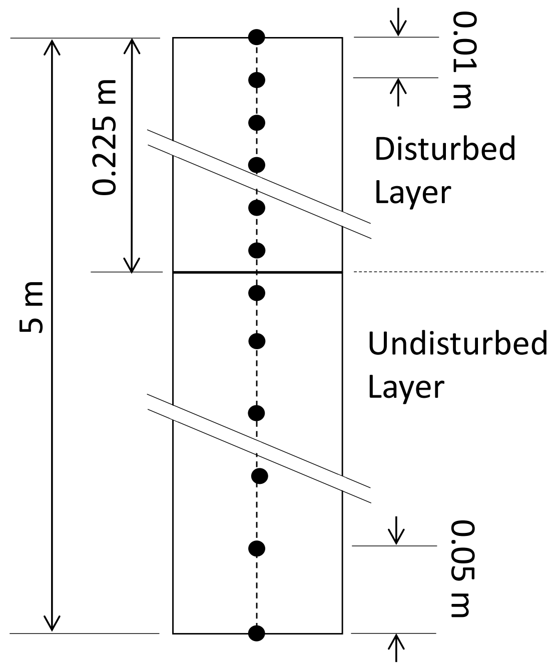

Figure 11. Soil profiled used in the HYDRUS-1D simulations. A has a uniform soil properties, and B and C have disturbed layer and undisturbed layer.

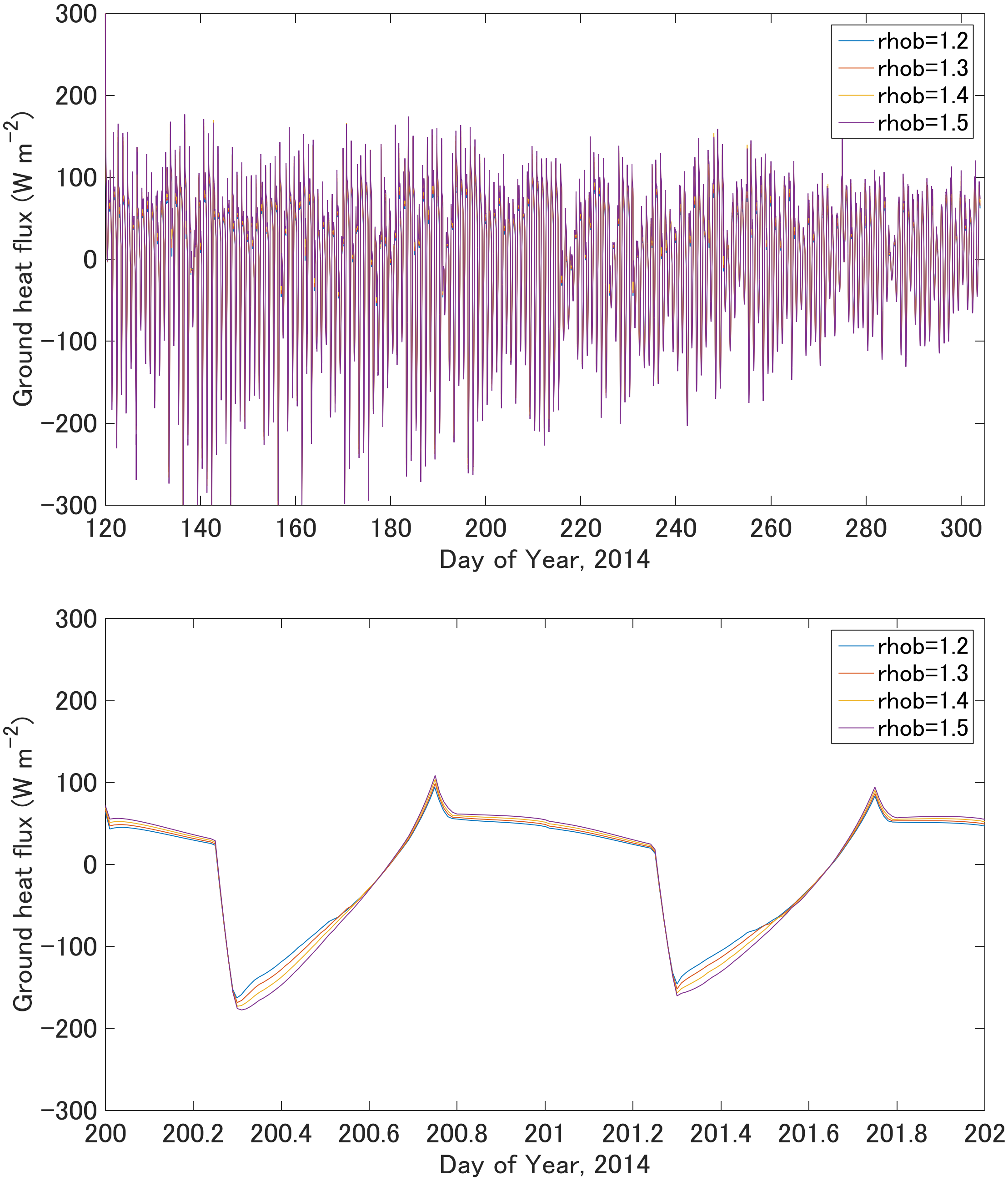

Figure 12. Simulated ground heat flux; positive values indicated downward heat flux. Top: May through October, bottom: day of year 200 to 202. Legends indicate bulk density (rhob) in Mg m^{-3}.

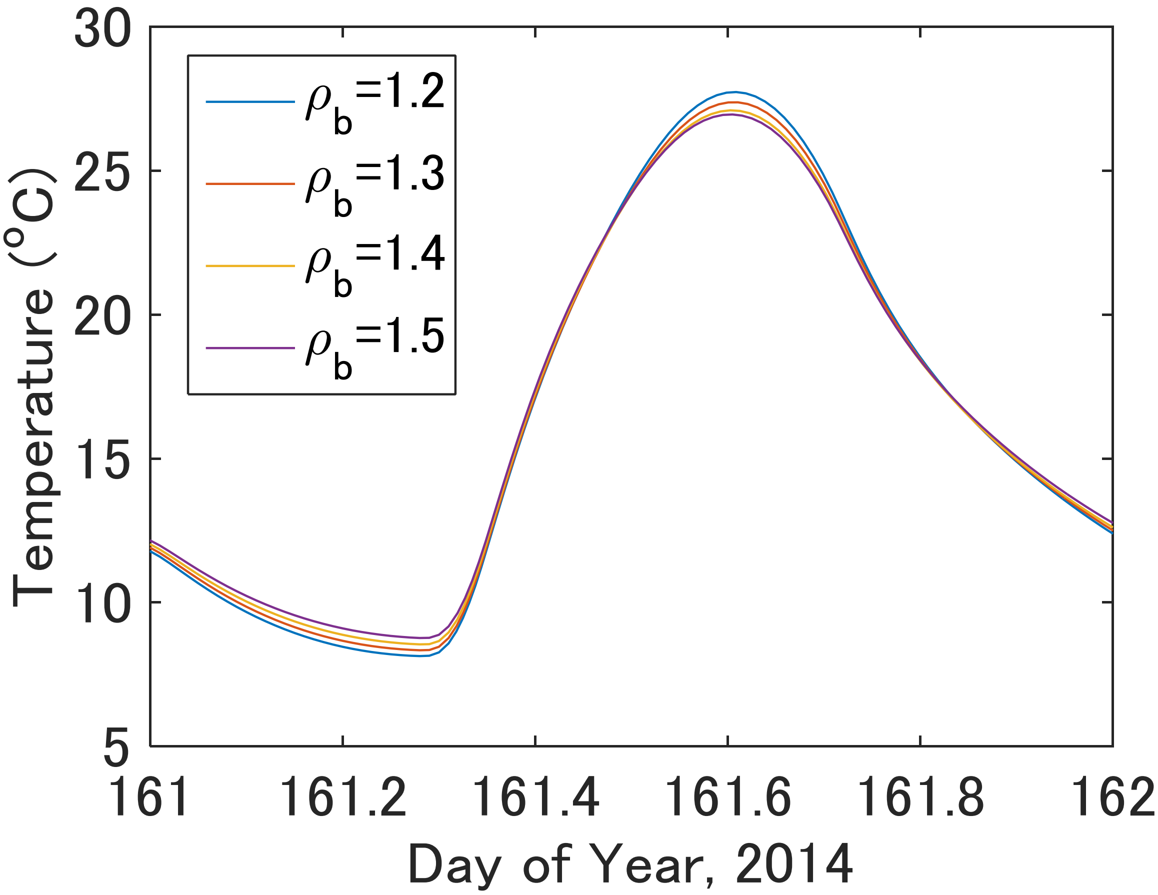

Figure 13. Simulated daily soil temperature at 5 cm soil depth. Legend indicates bulk density (ρ_b) in Mg m^{-3}.

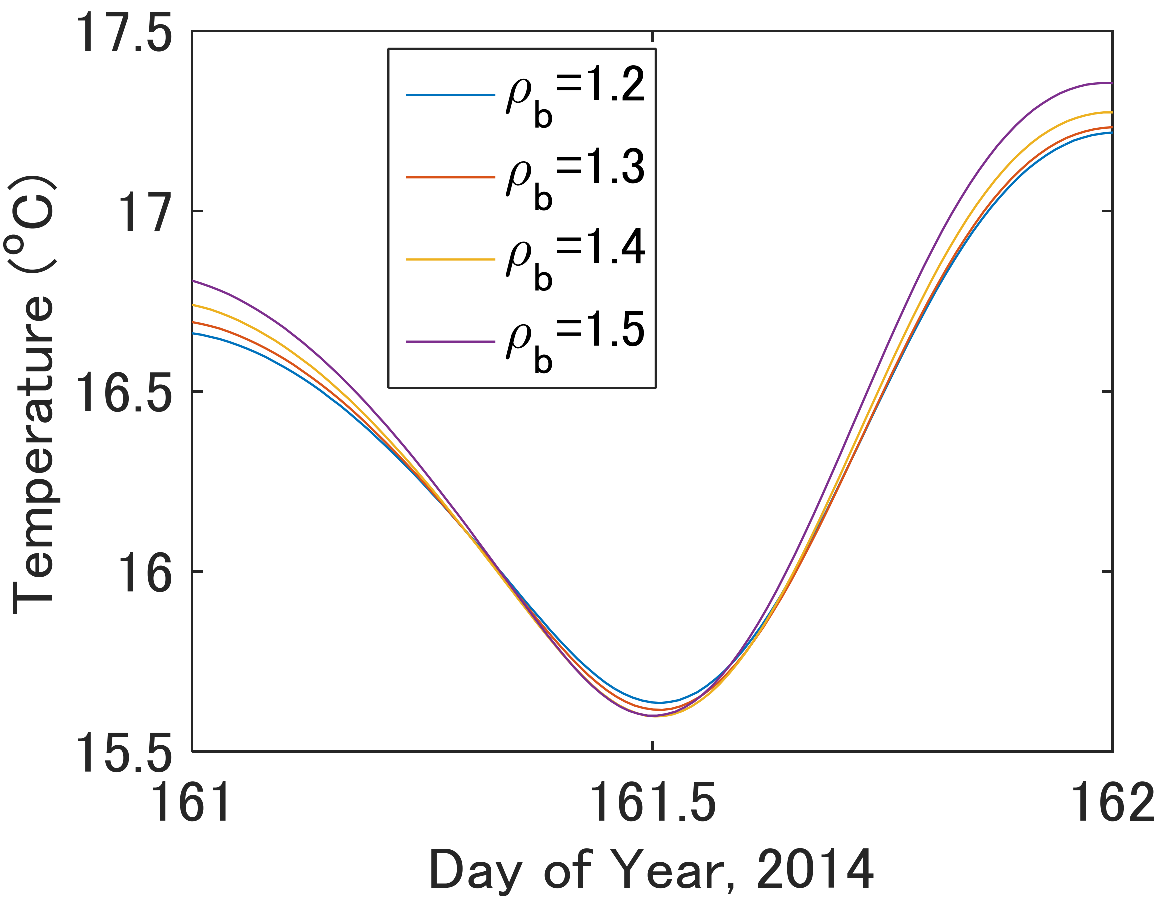

Figure 14. Simulated daily soil temperature at 30 cm soil depth. Legend indicates bulk density (ρ_b) in Mg m^{-3}.

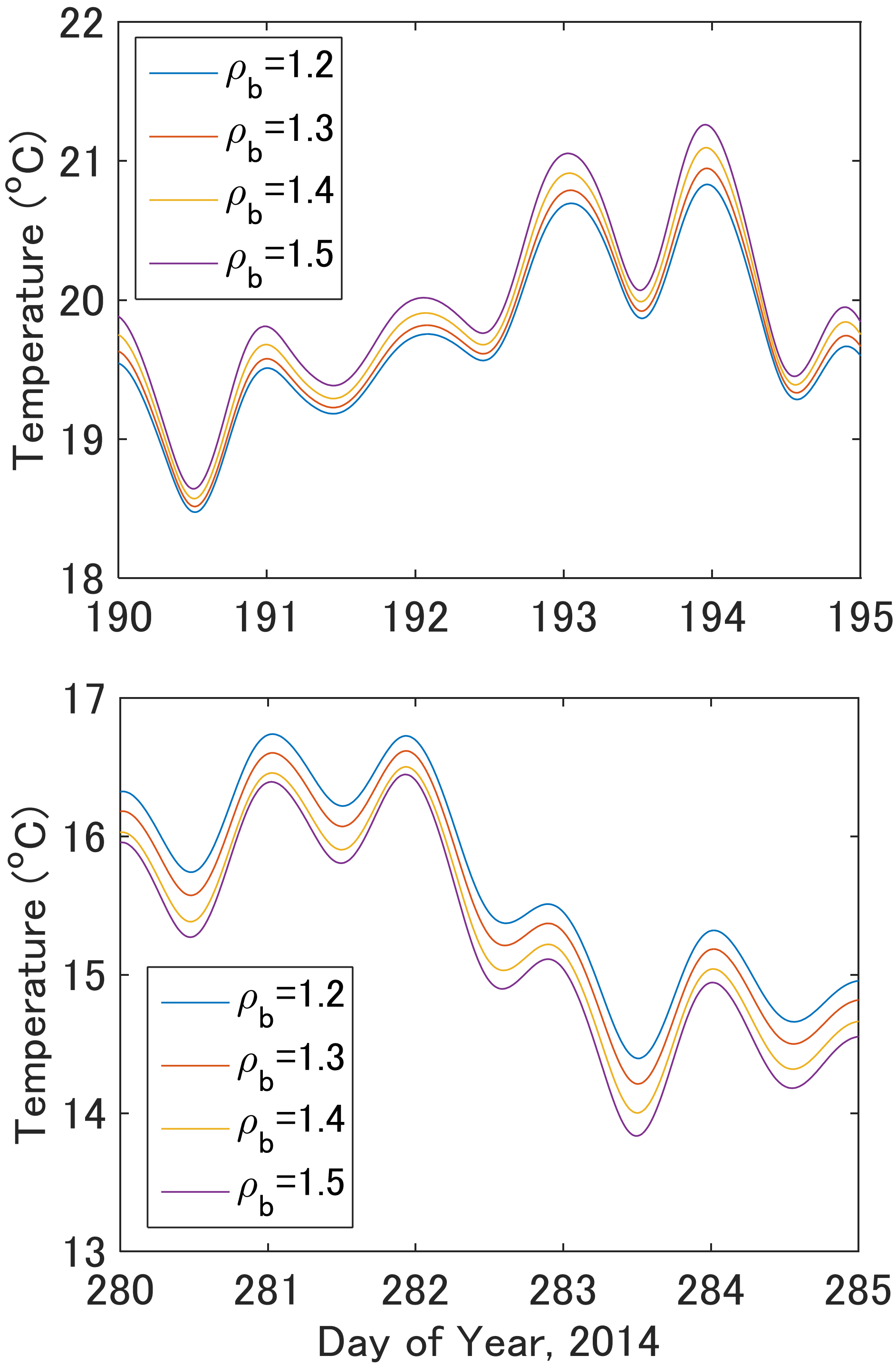

Figure 15. Simulated seasonal soil temperature at 30 cm soil depth. Top: summer, bottom: fall. Legend indicates bulk density (ρ_b) in Mg m^{-3}.

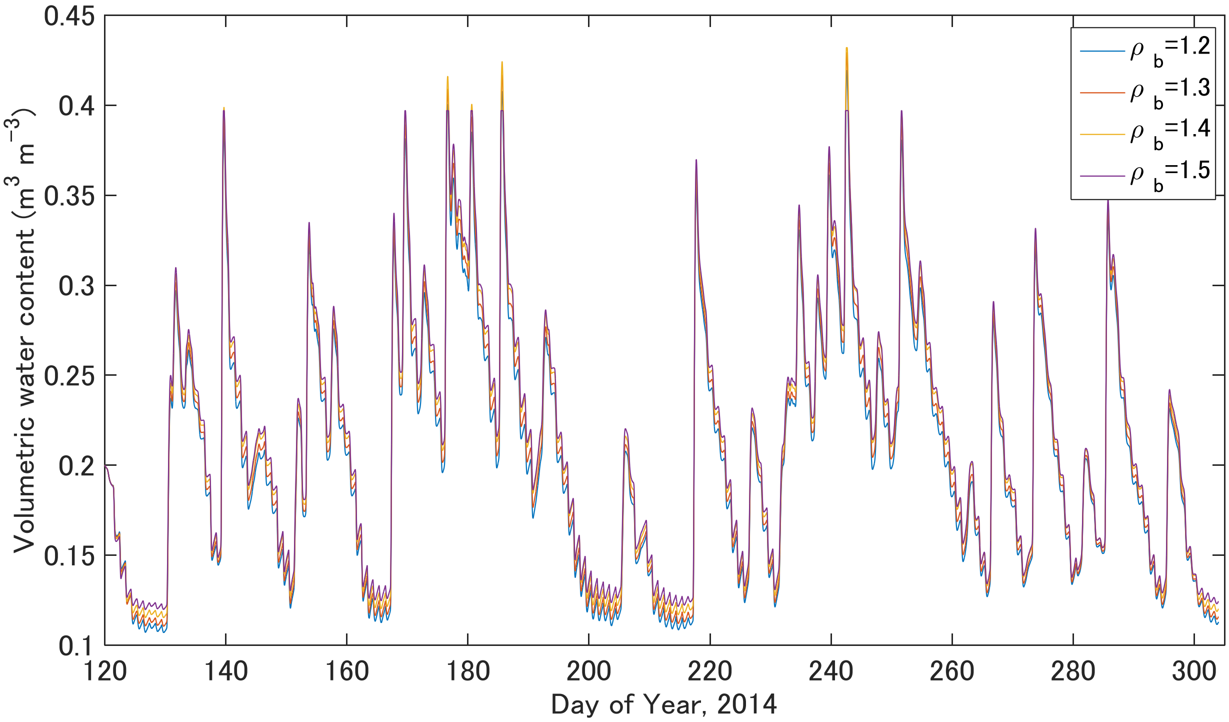

Figure 16. Simulated seasonal soil water content at 5 cm soil depth. Legend indicates bulk density (ρ_b) in Mg m^{-3}.

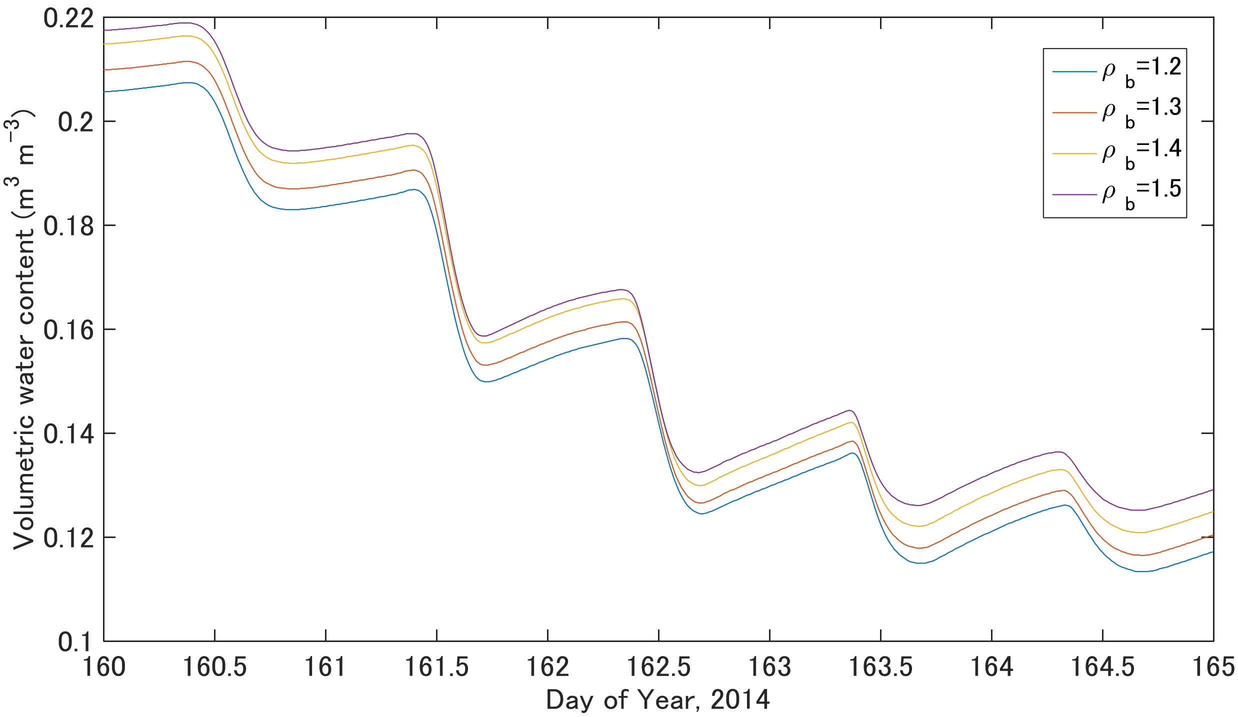

Figure 17. Simulated soil water content at 5 cm soil depth during a drying event. Legend indicates bulk density (ρ_b) in Mg m^{-3}.